UCC

University College Cork, Ireland
Coláiste na hOllscoile Corcaigh

Exploring a New Transmission Window for Telecommunications in the 2 µm Waveband

N. Kavanagh[1], *Member, IEEE,* M. Sadiq[1], K. Shortiss[1], H. Zhang[1], K. Thomas[1], A. Gocalinska[1], Y. Zhao[1], E. Pelucchi[1], P. O'Brien[1], F. H. Peters[1], B. Corbett[1] and F.C. Garcia Gunning[1], *Member, IEEE*

[1] Tyndall National Institute, University College Cork, Cork, Ireland

Tel: (00 353 21) 490 4872, e-mail: niamh.kavanagh@tyndall.ie

ABSTRACT

In this paper, we will demonstrate the possibility of opening a new telecommunications transmission window around the 2 µm wavelength, in order to exploit the potential low loss of hollow-core photonic bandgap fibers, with the benefits of significantly lower non-linearity and latency. We will show recent efforts developing a dense wavelength division multiplexing testbed at this waveband, with 100 GHz spacing wavelength channels and 105 Gbit/s total capacity achieved.

Keywords: new wavelength window, 2µm, arrayed waveguide grating, modulator, high capacity systems.

1. INTRODUCTION

The ever-increasing number of internet users and devices-per-user, combined with the popularization of video-streaming services, is driving today's telecommunications networks towards capacity limits, causing concern in the optical communications community about a potential "capacity crunch" as soon as the year 2020 [1]. Traditionally, optical communications R&D has focused on transmission in the C-band due to the minimum loss (~ 0.2 dB/km [2]) of standard single-mode fibers (SMFs) around 1.55 µm and the availability of Erbium-doped fiber amplifiers (EDFAs) in this waveband. However, fundamental propagation properties, such as loss and non-linearities, will inevitably limit the total capacity of SMFs [3]. These limitations have stimulated interest in new types of fibers which would allow for fundamentally higher capacities. Much research in recent years has been dedicated to developing multi-core and multi-mode fibers for this purpose, with record capacities [4].

However, other types of fibers, namely hollow-core photonic bandgap fibers (HC-PBGFs), may offer promising improvements which warrant investigation. HC-PBGFs consist of a unique honeycomb-like microstructure which confines light within a hollow core. The reduced interaction (of light) with the material (of the fiber) results in several encouraging advantages (over SMFs), such as a potential 1000-fold reduction in nonlinearity [6], near-vacuum latency and a predicted loss as low as 0.1 dB/km [5]. However, this minimum loss is located around 2 µm rather than 1.55 µm. Thus, these improvements require shifting signal transmission from the conventional C-band to the 2 µm wavelength region. Nonetheless, while these fibers offer several benefits, the realization of optical communications in this new wavelength region hinges on the availability of telecom-grade components, such as lasers, optical amplifiers, filters and detectors.

Table 1. *Capacity highlights*

Year	#Channels	Modulation	Modulation format	Data rate per channel (Gbit/s)	Total capacity (Gbit/s)	Ref
2012	1	1 x ext	NRZ-OOK	8	8	[8]
2012	4	1 x ext 3 x dir	NRZ-OOK BPSK FAST OFDM	8.5 5	20	[9]
2014	8	4 x ext 4 x dir	NRZ-OOK 4ASK FAST-OFDM	12.5 8.3	81	[11]
2014	1	1 x dir	64QAM OFDM	30	30	[12]
2015	8	4 x ext 4 x dir	NRZ-OOK 4ASK FAST-OFDM	15.7 10	100	[13]
2016	7	7 x ext	NRZ-OOK	15	105	this paper

In 2012, we demonstrated the first data transmission at 2 µm [8, 9]. This milestone achievement was the result of a Europe-wide effort (FP7 MODEGAP), which combined the HC-PGBF with advancements in semiconductor-laser technologies [4] and the availability of high-gain, low-noise Thulium-doped fiber amplifiers (TDFAs) [7]. With an operational testbed in place, many breakthroughs were subsequently achieved, such as wavelength division multiplexing (WDM) transmission [9], the implementation of advanced modulation formats [11] and the development of a wide range optical components [13]. Table 1, for example, highlights the evolution of 2µm systems in terms of capacity: growing from single-channel operation (with a limited 8 Gbit/s) to a complex WDM system with record capacities of over 100 Gbit/s [13]. In this paper, we present a WDM system with a total capacity of 105 Gbit/s. We will focus on the development of two particular InP-based devices enabling such 2 µm systems: a modulator and an arrayed waveguide grating (AWG), the latter to be used as a WDM filter. We will also discuss further increasing capacity in a dense WDM scenario.

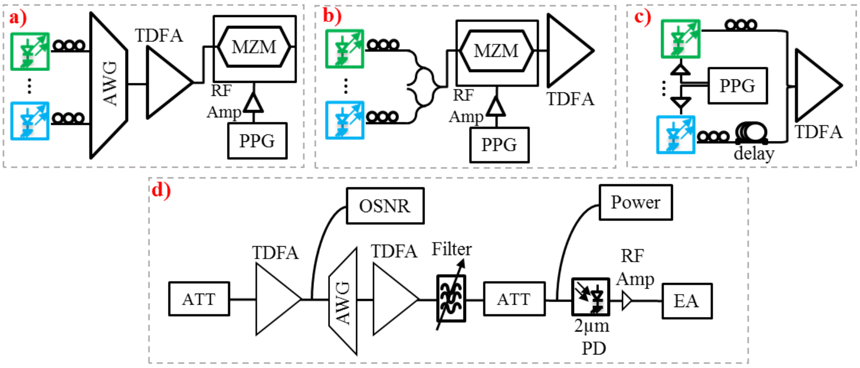

Figure 1 (a) *Tx with AWG as MUX. & LiNbO$_3$ MZM* ***(b)*** *Tx with standard combiners & InP MZM* ***(c)*** *Tx with DM lasers* ***(d)*** *Rx with AWG as de-mux. In all cases, signals transmitted over 1.15 km of HC-PBGF.*

2. TESTBED at 2µm

Building an operational testbed requires a whole suite of components capable of operating in this new wavelength region. Fig. 1 exemplifies the different transmitter (Fig.1 a - c) and receiver (Fig.1 d) configurations implemented recently. In the transmitter (Tx), while fiber couplers can be used to multiplex channels (Fig. 1 b, c), as the number of lasers increases the overall loss incurred will likewise increase. Hence, utilizing an AWG as a multiplexer (MUX), with the precise wavelength spacing required (e.g. 100GHz) is of immediate interest, as in Fig. 1a. (The AWG is discussed in further detail in the section below.) In addition, due to the strain on devices at this longer wavelength, many tend to exhibit relatively high losses. Thus, optical amplification (in the form of TDFAs) is required throughout the testbed. Modulation can be achieved either by using an external modulator, such as a Mach-Zehnder modulator (MZM), as per Fig. 1a, b, or directly modulating (DM) lasers, as per Fig. 1c.

The schematic of the receiver (Rx), shown in Fig. 1d, is more similar to that of a conventional 1.5 µm WDM system. The pre-amplified receiver consisted of a variable attenuator (ATT) which allowed for adjustment of the optical signal-to-noise-ratio (OSNR). For coarse WDM, channel selection was performed by a narrow-band filter (1.6 nm). In order to move to denser WDM and maintain sufficient channel isolation, a second packaged AWG was added to provide further filtering. Due to the inherent loss of the AWG, an additional amplifier was used between both filters, and the AWG was thermally tuned to ensure optimal filtering of the channel-under-test. After filtering, a second variable attenuator was placed before the (commercially-available) InGaAs photodetector (PD), and was adjusted to guarantee fixed power levels at the PD for all wavelengths, prior to error analysis (EA).

2.1 Arrayed Waveguide Grating

Although initially the need for an AWG was motivated by filtering requirements in the receiver, it was subsequently used in the transmitter to combine tightly-spaced WDM channels. Both AWG devices were designed, developed and packaged in-house [15]. The structure was grown by metal-organic vapor epitaxy (MOVPE) and was composed of a lattice-matched $In_{0.81}Ga_{0.19}As_{0.415}P_{0.585}$ quaternary, interleaved and capped by undoped InP layers. Mode leakage was reduced by using an n-doped InP substrate. Interchanging InGaAsP with the InP layers minimizes the total thickness of the quaternary and expands the mode. The waveguide was designed to have a large transverse mode-size of 3.6 µm, to minimize the impact of optical coupling to single-mode fiber at 2 µm. A 20-channel cyclical AWG with channel-spacing of 100 GHz was designed, with 164 waveguides (of 3.5 µm thickness and a group refractive index of 3.27) used to disperse the light. The radius of curvature was restricted to 1 mm to minimize the bend loss and prevent higher-order mode excitation, resulting in a chip size of 13 x 7 mm.

The chip was packaged in a housing with a single-channel lensed fiber input and a 10-channel fiber output array, with specialty fiber from OFS (ClearLite 1700 20) used. The fiber-packaged sub-assembly was then enclosed in a metal casing which included an integrated Peltier device for temperature control, with thermal dependence recorded to be 0.108 nm/^{0}C. Adjacent crosstalk of >18 dB between channels was measured, with an average insertion loss per channel of ~18 dB. This relatively high insertion loss can be attributed to mode mismatch between the optical fiber in the InP-based AWG at the input and output of the device. The thermal characterization of the receiver AWG was fine-tuned and temperature control was strictly maintained to accurately align with the channel-under-test, as per Fig.2a. In this figure, the black dotted line depicts the six WDM channels, separated by 100 GHz. Each colored line represents adjacent channels of the AWG output array, set at different temperatures (ranging from 16 – 17.5 ^{0}C) in order to optimize filtering for each channel.

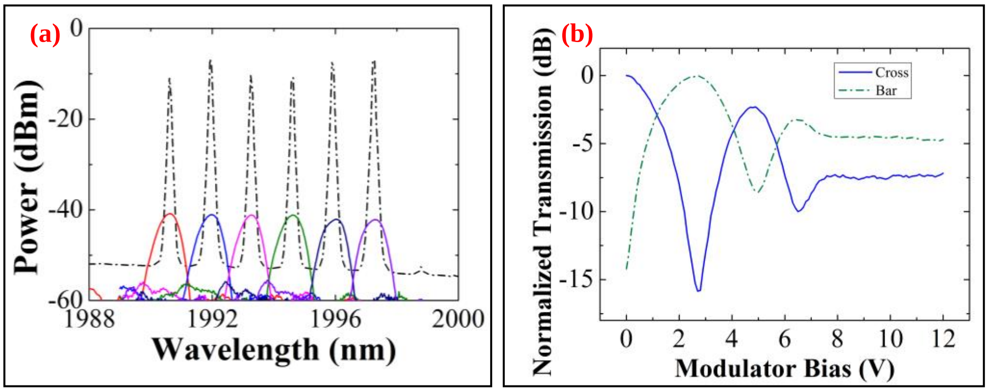

Figure 2 (a) *Receiver AWGr (de-multiplexer) thermal characterisation* ***(b)*** *DC transmission response of the InP MZM (with TWE length 2 mm) for both outputs: cross and bar, illustrating Vπ of 2.7 V.*

2.2 Modulator

It is not an easy task to find high-performance modulators at 2 µm. Commercially-available $LiNbO_3$ modulators are not only limited in bandwidth, but also suffer from large switching voltage (Vπ ~ 9-11 V). In addition, these devices have a large foot-print, suffer from bias point instability and are unsuitable for photonic integration. In order to improve the modulator performance and to move towards photonic integration at 2 µm, we developed an Indium Phosphide (InP) based MZM [14], based on the widely used travelling-wave-electrode (TWE) approach to achieve lower Vπ and high electro-optic bandwidth. Modulation in InP MZMs is generally achieved using refractive index change through the quantum-confined Stark Effect (QCSE), in intrinsically un-doped multiple quantum well (MQW) layers. These un-doped layers are interleaved between p and n-doped sections to form a p-i-n waveguide structure. The MQW layers are designed to exhibit an excitonic absorption peak at a wavelength shorter than (~ 0.15 µm below) the wavelength of operation. This ensures the minimum non-linear refractive index change due to higher absorption. Therefore, for 2 µm operation, a bandgap ~ 1.85 µm is desired. InGaAs has bandgap of ~ 1.65 µm when lattice matched to a suitable material, such as InP. By carefully introducing compressive strain in the quantum wells, this can be extended to longer wavelengths.

To split and combine the light in the interferometric paths (and maintain low splitting loss), the modulator chip was integrated with a 1 × 2 and 2 × 2 passive multi-mode interference (MMI) couplers at the input and output respectively. The modulator achieved a Vπ of 4 V and an electro-optic (EO) bandwidth of 9 GHz for 2 mm length TWE. The switching performance of the modulator was further improved by increasing the number of MQWs from 15 to 25. The increase in number of wells resulted in lower Vπ of 2.7 V due to higher EO overlap in the intrinsic region, without compromising the EO bandwidth performance i.e. 9 GHz. Fig. 2b depicts the DC transmission response of the modulator with a TWE length of 2 mm, for both the outputs of the MMI (referred to as cross and bar) with a Vπ of 2.7 V shown. The transfer function was measured at the wavelength of 1994.260 nm for TE polarized input light with the reverse bias voltage applied only to a single arm of the modulator. The slight imbalance between the output arms is due to a minor variation in MMI dimensions during fabrication. However, while the Vπ was reduced by 1.3 V, it was found that the insertion loss increased by nearly 4 dB. This could be attributed to a small shift in the absorption peak due to the increased number of QW, leading to increased absorption around 2 µm. Also, a dominant source of loss in the device is the fiber-to-chip coupling. This increase could be reduced by incorporating spot-size converters at the input and output of the device. This would result in much higher misalignment tolerance and could reduce the insertion loss by ~10 dB, which would be more comparable to devices currently operating at 1.55 µm [14].

3. SYSTEMS PERFORMANCE

Wavelength division multiplexing (WDM) is the first step towards a high-capacity system. We previously demonstrated coarse WDM [9], with the challenge of reducing channel-spacing to 100 GHz later resolved with the use of an AWG at the receiver [15]. Here, we show the results of implementing an AWG at the transmitter side as well, reaching 105 Gbit/s capacity, based on 7 x 15 Gbit/s NRZ-OOK data modulation, using a commercial $LiNbO_3$-based modulator and a pseudo-random bit-sequence (PRBS) sequence of 2^{31}-1. Fig. 3a shows the bit error rate (BER) performance against OSNR for all WDM channels after transmission over 1.15 km of HC-PBGF, with no evidence of an error floor. For a BER of $1x10^{-9}$, the average OSNR required was 26 dB, with a spread of 2 dB.

Thus, we have established that WDM with 100 GHz channel-spacing is possible at 2 µm. However, in order to optimize available bandwidth, increase capacity and move closer to replicating 1.55 µm telecommunication standards, the viability of reducing WDM channel-spacing to 50 GHz was investigated [16]. This was done by combining 6 x 12.5 Gbit/s NRZ-OOK externally-modulated lasers (referred to as the even-channels, as per Fig. 1a) and 2 x 8 Gbit/s directly-modulated lasers (odd-channels as per Fig. 1c), independently modulated with

NRZ-OOK from a second pulse pattern generator (PPG). The odd-channels were thermally tuned to emit at wavelengths in-between the even-channels, resulting in 50 GHz spacing in the transmission spectrum, as shown in Fig. 3b. It was ensured that the data from odd and even channels were completely de-correlated, before transmission through the fiber. The impact of 50 GHz channel-spacing was investigated by measuring the bit-error-rate (BER) of the even-channels before and after the odd-channels were switched on. It was expected that the reduced channel-spacing would result in an observable OSNR penalty. However, no such penalty was measured. It was surmised that, while 50 GHz channel-spacing can be achieved in terms of transmission, there remain several issues associated with the receiver, chiefly, better filtering techniques are necessary for sufficient channel isolation [16].

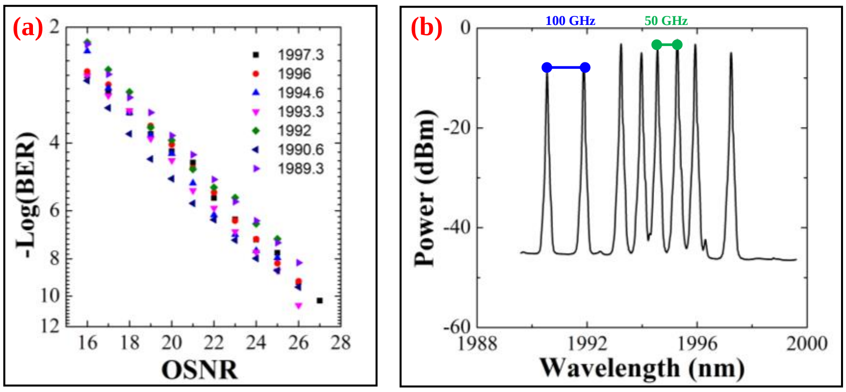

Figure 3 (a) *BER vs. OSNR performance for 7 x 15 Gbit/s NRZ-OOK externally-modulated channels with 100 GHz spacing, multiplexed by an AWG and transmitted over 1.15 km of HC-PBGF* ***(b)*** *Transmitted spectrum with 50 GHz channel-spacing*

4. CONCLUSION

In this paper, we discussed the development of an optical communications testbed at 2 µm, with particular focus on the design and performance of two InP-based devices: a modulator and an arrayed waveguide grating (AWG). We highlighted recent efforts in increasing the overall capacity of the system, evolving from single-channel to WDM with 100 GHz channel-spacing and record capacities of 100 Gbit/s transmitted over 1.15 km of HC-PBGF. Here we have shown a total capacity reaching 105 Gbit/s, addressing the challenges associated with further increasing the capacity to a dense WDM scenario (with 50 GHz channel-spacing), most critical of which are the available filtering techniques.

ACKNOWLEDGEMENTS

We would like to thank Eblana Photonics for providing the lasers and the Optoelectronics Research Centre, University of Southampton for providing the fiber and TDFAs for this experiment. We would like to acknowledge funding support from the Irish Research Council (GOIPG/2014/637), EU FP7 IP project MODEGAP (258033) and Science Foundation Ireland under CTVR (10/CE/I1853), IPIC (12/RC/2276) and (13/CDA/2103).

REFERENCES

[1] D. J. Richardson et al., *Science*, vol. 330(60002), pp. 327-328, Oct. 2010
[2] T. Miya et al., *Electronics Letters*, vol. 15(4), pp. 106-108, Feb. 1979
[3] A. D. Ellis et al., *J. Lightwave Technol.*, vol. 28(4), pp. 423-433, Feb. 2010
[4] D.J. Richardson et al., *Nat. Photon.* vol. 7(5), pp. 354-362, Apr. 2013
[5] P.J. Roberts et al., *Opt. Express*, vol. 13(1), 236-244, Oct. 2005
[6] C.M. Smith et al., *Nature*, vol. 424(6949), pp. 657-659, Aug. 2003
[7] Z. Li et al., *Opt. Express*, vol. 21(8), pp. 9289-9297, Apr. 2013
[8] M. N. Petrovich et al., *ECOC 2012*, Amsterdam, Holland, paper Th.3.A.5, Sept. 2012
[9] N. Mac Suibhne et al., *ECOC 2012*, Amsterdam, Holland, paper Th.3.A.3, Sept. 2012
[10] R. Phelan et al., *Photon. Technol. Lett.*, vol. 24(8), p. 652-654, Apr. 2012
[11] H. Zhang et al., *ECOC 2014*, Cannes, France, paper P.5.20, Sept. 2014
[12] Z. Liu et al., *ECOC 2014*, Cannes, France, paper Tu.4.3.5, Sept. 2014
[13] H. Zhang et al., *Optics Express*, vol. 23(4), pp. 4946-4951, Feb. 2015
[14] M. Sadiq et al., *J. Lightwave Technol.*, vol. 34(8), pp. 1706-1711, Apr. 2015
[15] H. Zhang et al., *Optics letters*, vol. 40(14), pp. 3308-3311, Aug. 2015
[16] N. Kavanagh et al., *CLEO US*, San Jose, USA, paper SF1F.5, June 2016